Microchim Acta (2015) 182:2329–2336
DOI 10.1007/s00604-015-1564-y

ORIGINAL PAPER

Proximity-based electrochemical biosensor for highly sensitive determination of methyltransferase activity using gold nanoparticle-based cooperative signal amplification

Zhang Zhang[1] · Shangchun Sheng[2] · Xianqing Cao[1] · Yiyan Li[3] · Juan Yao[1] · Ting Wang[1] · Guoming Xie[1]

Received: 14 February 2015 / Accepted: 3 July 2015 / Published online: 1 August 2015

Abstract We describe a turn-on electrochemical biosensor for the detection of methyltransferases (MTases) causing DNA adenine methylation. This biosensor is based on insertion, methylation-resistant cleavage, signal enrichment caused by gold nanoparticles (AuNPs), and a signal probe-dragging strategy. A double-stranded DNA (dsDNA) containing identical MTase and methylation-resistant endonuclease (Mbo I) sites was immobilized on the surface of a gold electrode via Au-S covalent binding. The surface was subsequently treated with MTase and Mbo I and then washed. Results revealed that the surface of the electrode contains methylated dsDNA and 12-base nucleotides residual. Depending on biotin-streptavidin interactions that enabled signal probes and nucleotide residue hybridization and AuNP enrichment, a large number of signal probes labeled with ferrocene (Fc) are captured by the electrode. Under optimal conditions, the differential pulse voltammetry signals of Fc tags (at a working voltage of 0.24 V vs. Ag/AgCl) are linearly related to the log of the MTase activity in the 0.1 to 40 U·mL^{-1} range. The dynamic range extends from 0.05 to 50 U·mL^{-1}, and the limit of detection is 0.024 U·mL^{-1} (at an S/N ratio of 3). The assay is well reproducible and highly selective. In our perception, this strategy provides a promising approach for simple, sensitive and selective detection of Dam MTase and may be extended to the determination of other MTase by exchanging the corresponding DNA.

Keywords Electrochemical DNA biosensor · Dam methyltransferase · Methylation-resistant cleavage · Insertion method · Dragging strategy

Introduction

DNA methylation is a major form of epigenetic gene regulation in prokaryotes and eukaryotes [1, 2]. Numerous of studies have proven that DNA methylation is associated with X chromosome inactivation, gene regulation and transposon silencing [3]. Aberrant DNA methylation is associated with multiple disease states, including Rett syndrome [4], autoimmune diseases [5] and multiple types of cancer [6]. The link between abnormal DNA methylation and cancer has been widely investigated; excessive and deficient methylation processes have been identified in diverse tumor types. Abnormalities in methyltransferase (MTase) activity usually occur far before other signs of malignancy manifest and thus can be used as basis to diagnose tumor in early stages.

Radioactive labeling with [methyl-^{3}H]-SAM [7] is a standard method to performs MTase activity assays. To avoid radioactivity contamination, researchers further developed other assays, including polymerase chain reaction (PCR)-based techniques [8, 9], gel electrophoresis, high performance liquid chromatography (HPLC) [10], light scattering [11], fluorescence method [12], and colorimetric assays [13]. Although these methods are non-radioactive, these methods

Electronic supplementary material The online version of this article (doi:10.1007/s00604-015-1564-y) contains supplementary material, which is available to authorized users.

✉ Guoming Xie
guomingxie@cqmu.edu.cn

[1] Key Laboratory of Laboratory Medical Diagnostics of Education, Department of Laboratory Medicine, Chongqing Medical University, Chongqing 400016, People's Republic of China

[2] The No.2 People's Hospital of Yibin, Sichuan 644000, People's Republic of China

[3] Department of Electrical and Computer Engineering, College of Engineering, University of Nevada, Las Vegas, NV 89154-4026, USA

show several drawbacks, such as time-consuming, laborious, and complicated processes. Additionally assays base on methylation-resistant cleavage confers protection of DNA sequence from digesting by corresponding restriction endonuclease [14]. Recently, electrochemical biosensors [15–17] overcame many of these drawbacks and showed a great potential to be a nonradioactive, fast-response, relatively low-cost, highly sensitive and portable biosensors for DNA adenine methylation (Dam) MTase detection.

An important challenge in the DNA biosensors is controlling the conformations, orientation and spatial distribution of the immobilized DNA probes, which impact the sensitivity, selectivity and reproducibility of these sensors. Over a long decade, backfilling method [18–20] for DNA probe immobilization, which shoehorned alkanethiol into the interspaces between preassembled DNA monolayer, has been the prominent way for the construction of DNA biosensor interface. However, recent studies [21] showed that DNA molecules on the surface of a gold electrode prepared by backfilling method have the tendency to form aggregations thus can't offer efficient space for enzyme reaction. Insertion method prepared by inserting thiolated DNA into a preformed alkanethiol monolayer can yield a more uniform surface at molecular scale than backfilling method. To the best of our knowledge, the DNA biosensor fabricated via insertion method to make DNA probes more uniform and give sufficient space for enzyme digestion has not yet been reported.

In this study, a turn-on electrochemical assay was developed to detect Dam MTase. Dam MTase was used as a model target to catalyze adenine methylation in 5′-GATC-3′ sequence based on methylation-resistant enzymatic reaction, AuNP-dependent enrichment of redox-active moieties, dragging strategy, and background suppression. As shown in Scheme 1, double-strand DNA (dsDNA) S1/S2 was immobilized on the surface of a gold electrode via Au-S bond, with a biotin moiety at the 5′ end of S1 to further introduce signaling reporters. In the absence of Dam MTase, dsDNA and biotin tag were cleaved by endonuclease; as a result, subsequent signal reporter reactions were prevented and background current were suppressed. In contrast, when methylation blocks the restriction enzyme cutting site to some extent, Mbo I was unable to cleave the methylated dsDNA thus reserve biotin tag, while the unmethylated dsDNA is cleaved by Mbo I and leave a 12 nucleotides residue in length on the electrode after washing steps. The products left on the electrode were methylated dsDNA and 12-base length nucleotides which were used as a fixer to be hybridized with signal probe. Similar results were verified by other works [22, 23]. With a large number of signal probes attached to AuNP captured by DNA S1 on the electrode through biotin-streptavidin high affinity interaction, the electrochemical signal can be significantly amplified. Nonetheless, due to the electrostatic repulsion between the signal probe and the gold electrode modified with DNA, the ferrocene (Fc) tags labeled signal probe may fail to contact with electrode efficiently. To solve this problem, the signal probe was designed to hybridize with DNA S1 residue on the electrode. In this way, Fc tags can be dragged closer to the electrode and further facilitate interfacial electron transfer. The background signal was mainly derived from the hybridization between the 12-base length nucleotides residue and streptavidin-gold nanoparticle-signal probe (SA-AuNP-SP). Through optimizing the length of signal probe complementary to DNA S1 residue can we obtain a higher signal to noise ratio thus enhance sensitivity.

Experimental

Reagents

Ultrapure water was purified using a Milli-Q system (≥18 MΩ·cm, http://www.emdmillipore.com/US/en) and used throughout the experiment. All oligonucleotides were synthesized and purified through high-performance liquid chromatography by Shanghai Sangon Biotechnology Co. (Shanghai, China, http://www.sangon.com/); the sequences are listed in Table 1. Hydrogen tetrachloroaurate trihydrate ($HAuCl_4 \cdot 3H_2O$), Streptavidin (SA) and 6-hydroxy-1-hexanethiol (MCH) were obtained from sigma-aldrich (St.louis, USA,http://www.sigmaaldrich.com/). Dam, M.Sss I, Hpa II, and Hae III MTases methyltransferases and Mbo I restriction endonuclease were purchased from New England Biolabs (Ipswich, MA, http://www.neb.com/). All the other chemicals were of analytical grade and used without further purification.

Apparatus

A CHI660D electrochemical work station (Shanghai, China, http://www.chinstruments.com/) was employed for all experiments. A normal three-electrode system including a Pt wire auxiliary electrode, an Ag/AgCl reference electrode and a 3 mm diameter gold disk electrode as the working electrode (Wuhan, china, http://gaoshiruilian.labscn.com.cn/) was used thought this work. Transmission electron microscope (Hitachi-7500, Japan http://www.hitachi.com/), UV-vis Spectrophotometer (Mapada-1600PC, China, http://mapada.foodmate.net/), and Nano-DROP1000 (Thermo, USA, http://www.thermoscientificbio.com/) were used to characterize the fabricated AuNP and SA-AuNP-SP.

The fabrication of SA-AuNP-SP

AuNP solution(20 nm in diameter) was prepared using a previously described method. First, 50 mL of $HAuCl_4$ solution (0.01 %, *m/v*) was boiled with vigorous stirring. Second, 2 mL

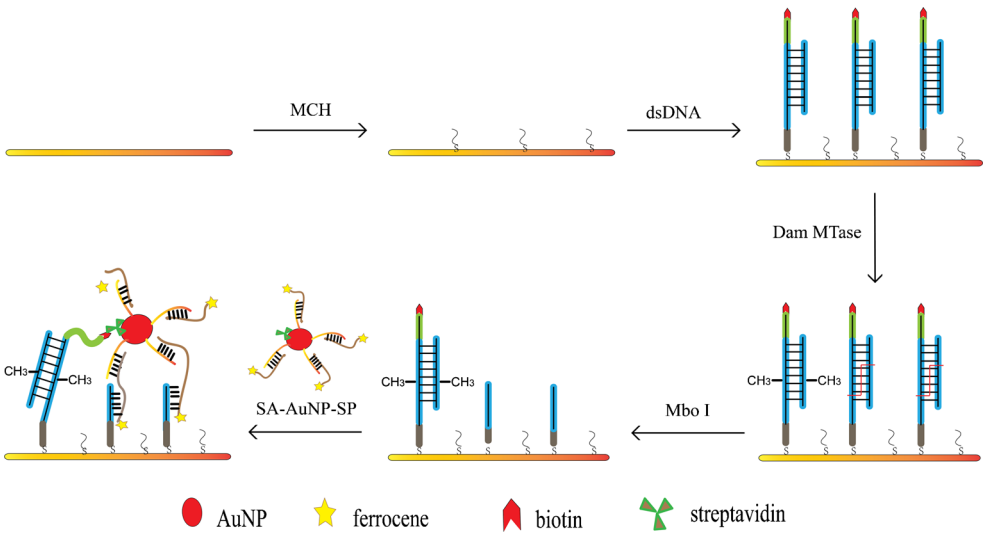

Scheme 1 Schematic illustration of sensing system for the detection of Dam MTase activity by using methylation-resistant cleavage coupled with proximity-based cooperative amplification. The washing buffer was used between the main steps of the fabrication process

of trisodium citrate solution (1 %, *m/v*) was rapidly added to the boiling solution. AuNPs were formed when the color of the solution changed from pale yellow to wine red. The solution concentration was approximately 0.4 nM, which was calculated according to Lambert-beer law with an extinction coefficient of 5.41×10^8 M^{-1} cm^{-1} at λ=520 nm [24]. The as-prepared AuNP were densely functionalized with thiol-modified oligonucleotides in accordance with established procedures but with slight modifications [25–27]. In brief, 10 μL of 100 μL thilolated DNA was mixed with 1 mL of AuNP and incubated at 4 °C for 16 h with gentle stirring. Subsequently, 10 μL of 1 % SDS was injected with shaking at room temperature for 1 h to stabilize AuNP. Afterward, 100 μL of 1 M NaCl solution was slowly added and aged for 12 h. Excess thiolated oligonucleotides were removed by subjecting to centrifugation thrice. At last, the precipitate was re-suspended in 1 mL of phosphate buffer (pH 7.4) for 1 h on a vortex stirrer and then incubated with 50 μL of 10 nM streptavidin with gentle shaking for 1 h to ensure that streptavidin-to-AuNP ratio was approximately 1:1, which allows SA to conjugate with AuNP via noncovalent adsorption [28]. Finally, the DNA-AuNP conjugates were mixed with 10 μL of 100 μM signaling probe. After incubation for 1 h and remove excess reagents, the wine-red SA-AuNP-SP complexes were obtained.

Table 1 Sequences of the designed oligonucleotides

Oligonucleotides	Sequences(5′ to 3′)
DNA S1	SH-GTCTGCTCTCAAGATCCCACGACGCTCT ATAGAC-biotin
DNA S2	AGAGCGTCGTGGGATCTTGA
SP1	AGTTCATAAGCACTTCGATTGAGA-Fc
SP2	AGTTCATAAGCACTTCGATTGAGAG-Fc
SP3	AGTTCATAAGCACTTCGATTGAGAGC-Fc
SH-DNA	TCGAAGTGCTTATGAACTCGAGATCTT

Electrochemical biosensor fabrication and measurement

Biosensors were fabricated using standard approaches. Briefly, gold disk electrodes were prepared by polishing with 0.3 and 0.05 μm alumina slurry, followed by sonication in ultrapure water, ethanol and ultrapure water for 5 min respectively. After this treatment, the electrode was cleaned up in piranha solution (1:3 H_2O_2/H_2SO_4 by volume) for 10 min and thoroughly rinsed with distilled water. (CAUTION: Piranha solution can react violently with organic equipment and should be handled with personal protective equipment.) Finally, electrochemical cleaning was conducted at the electrode with 30 successive CV scans from 0.2 to 1.6 V in 0.5 M H_2SO_4, further rinsed in distilled water and dried with nitrogen.

As shown in Scheme 1, a homogeneous monolayer preparation was conducted via the insertion approach. The cleaned electrode was initially immersed in MCH solution for 20 min and washed with washing buffer (100 mM phosphate buffer pH 7.4) at room temperature to provide sufficient space treat dsDNA with Dam MTase and Mbo I; afterward, 10 μL 1 μmol DNA S1/S2 solution for 16 h at 4 °C (S1 and S2 were initially mixed at 1:1, annealed by heating at 95 °C for 5 min, and slowly cooled down to room temperature). Then the electrode was rinsed thoroughly with washing buffer. Subsequently, the electrode was incubated with 10 μL of Dam MTase solution at different concentrations by using a CutSmart buffer containing 80 μL SAM and various amounts of Dam MTase at 37 °C for 2 h. After methylation was complected, the electrode was washed thoroughly to terminate the methylation reaction and then dried with nitrogen. Afterward, the electrode was immersed in 10 μL of Mbo I for 2 h at 37 °C and coated with 10 μL of SA-AuNP-SP solution at room temperature for 10 min. The resulting electrode was washed with washing buffer and kept in this buffer for 30 min to facilitate DNA hybridization.

Electrochemical measurements were performed on a CHI 660D electrochemical workstation at room temperature. In electrochemical experiments, cyclic voltammetry (CV) scans were performed at a scan rate of 100 $mV \cdot s^{-1}$ in a potential window from −0.2 to 0.6 V. Differential pulse voltammetry (DPV) was recorded from 0 to 0.4 V under the following parameters: increment potential, 0.005 V; pulse amplitude, 0.05 s; pulse width, 0.05 s; pulse period, 0.5 s; and quiet time, 2 s. The detection buffer was 20 mM phosphate buffer (pH 7.4) containing 0.1 M $KClO_4$ (a weak nucleophile, used as the electrolyte to avoid the instability of the ferrocenium, which is the oxidized form of ferrocene). All measurements were conducted at room temperature (25 °C). The reported DPV curves were background-subtracted to the base line.

Results and discussion

Electrochemical characterization of the prepared biosensor

Cyclic voltammetry (CV) and electrochemical impedance spectroscopy (EIS) [29] were performed to characterize biosensor fabrication. As shown in Fig. 1b, electron-transfer resistances (Ret) of different modified biosensors were recorded. Figure 1a presents the corresponding CV curves. The peak current density of CV was obvious in the bare electrode (Fig. 1a, curve a), and Ret was almost a straight line (Fig. 1b, curve a). After the gold electrode was blocked by MCH, because MCH prevented electron transfer, Ret increased (Fig. 1b, curve b), and the peak current density of CV decreased (Fig. 1a, curve b). peak current intensity (Fig. 1a, curve c) decreased and Ret (Fig. 1b, curve c) increased after DNA S1/S2 self-assembled on the electrode and electrostatic repulsion occurred between the negatively charged deoxyribose-phosphate backbone of dsDNA and $Fe(CN)_6^{3-/4-}$. The current response density of CV increased (Fig. 1a, curve d), whereas Ret (Fig. 1b, curve d) significantly decreased when 10 μL of 50 $U \cdot mL^{-1}$ Mbo I endonuclease was added. The degree of change in current response density (Fig. 1a, curve e) and Ret (Fig. 1b, curve e) when dsDNA was treated with Dam MTase and Mbo I was small because dsDNA was protected from endonuclease through methylation. CV and EIS data indicated that the electrochemical biosensor was successfully fabricated.

Impedance data were further fitted according to a Randless equivalent circuit based on ZSimpWin version 3.10. The equivalent electrical circuit consisted of an active electrolyte resistance (R_s) in a series with a constant phase element (CPE) and an impedance of faradaic reaction (Ret) in parallel with Warburg impedance (Z_W). Figure 1c shows that curve c fitted (Fig. 1b) to the equivalent circuit is consistent with measurement results in the whole frequency range; this result indicated that Ret can be used to monitor changes in electrodes.

Characterization of AuNP and SA-AuNP-SP

AuNP and SA-AuNP-SP were characterized through TEM and UV-vis absorption spectrometry. In Fig.S1a (Electronic Supplementary Material), the nanoparticles displayed spherical and homogeneous dispersion. UV-vis absorption spectra was adopted to confirm the successfully fabrication of SA-AuNP-SP. As shown in Fig. S1b, the surface plasmon resonance peak of SA-AuNP-SP exhibited a spectral red shift [24].

Optimization of experimental conditions

Various experimental parameters, such as MCH concentrations, signal probes, SAM concentrations, and Mbo I concentrations, were optimized to obtain the most efficient DNA biosensor performance. These experiments were conducted using 20 $U \cdot mL^{-1}$ Dam MTase.

To make the probe more homogeneous on electrode as well as give efficient space for enzymatic cleavage. The

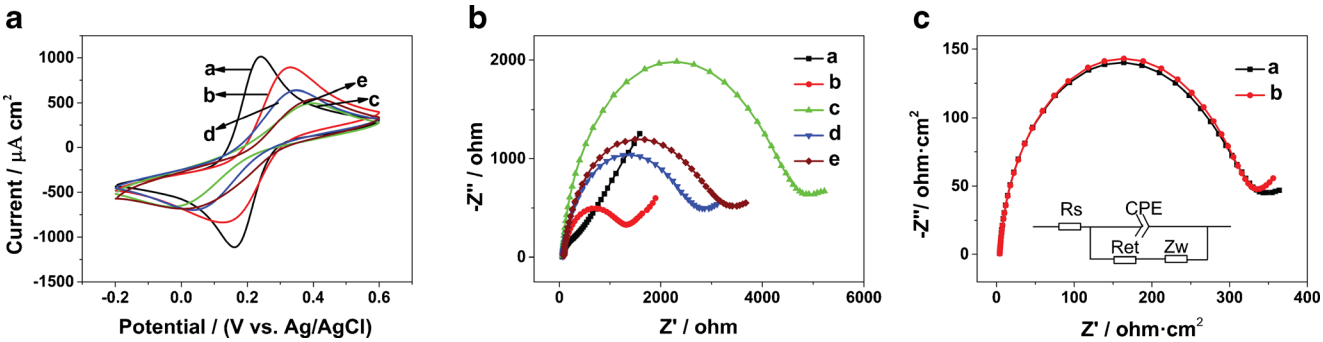

Fig. 1 Cyclic voltammetry (**a**) and EIS Nyquist plots of impedance spectra (**b**) at (*curve a*) the bare gold electrode; (*curve b*) MCH/Au; (*curve c*) DNA S1/S2 /MCH/Au; (*curve d*) DNA S1/S2/MCH/Au/Mbo I; (*curve e*) DNA S1/S2/MCH/Au/MTase/ Mbo I. The concentrations of MTase and Mbo I are 40 $U \cdot mL^{-1}$ and 50 $U \cdot mL^{-1}$ each. **c** Experimental (*curve a*) and fitted experimental Nyquist plots (*curve b*) of impedance spectra. The *inset* shows the equivalent circuit used to model impedance data. All the experiments were carried out in 0.1 M phosphate buffer (pH 7.0) containing 5 mM $[Fe(CN)_6]^{3-/4-}$ and 0.1 M KCl

concentrations of MCH using insertion approach to passive electrode were optimized to obtain the best analytical performance. As shown in Fig. 2, Ret increased as MCH concentration increased. When immobilized with DNA S1/S2, Ret increased further as the degree decreased. This result is possible because the decreased amount of dsDNA immobilized on the electrode reduced the repulsion between deoxyribose-phosphate backbone and $Fe(CN)_6^{3-/4-}$. Digestion reaction induced a decrease in Ret when dsDNA was treated with endonuclease. The enzyme digestion efficiency of dsDNA increased from 7.9 to 62.0 % when MCH concentration increased and reached the maximum concentration of 100 μM (Table S1). Thus, 100 μM was selected as optimal experimental condition.

The approach of the Fc tags to the electrode surface depends on the hybridization between signal probe and a 12-base nucleotide residue of S1 on the electrode after enzymatic cleavage occurred. Three different signal probes containing 6, 7, and 8 nucleotides residue complementary to 12-base nucleotide S1 residue were designed to verify the benefits of this strategy and improve biosensor performance. Under optimal conditions, Gibbs free energy change (ΔG) and melting temperatures (T_m) were calculated using UNA Fold software [30] to determine hybridization between S1 residue and SP1, SP2, and SP3 (see Table S2). In theory, S1 residue is unable to hybridize with SP1 and SP2 at 25 °C because of the low affinity while the hybridization with SP3 is achievable. Figure 3 shows a comparison between signal and background response of this system to 6, 7, and 8 complementary nucleotides. In the case of SP1 (Fig. 3a), the current peak intensity was 42.5 % of SP2 (Fig. 3b) while the background signals of both were negligible. Data of SP1 and SP2 indicated that signal to noise ratio is likely enhanced if signal probe contains more nucleotides complementary; with more nucleotides, Fc tags are closer to the electrode, thereby improving biosensor performance. However, further extension of SP3 complementary region slightly enhanced signal intensity; conversely, background signal strongly increased, resulting in a deteriorated signal to noise ratio (Fig. 3c). The reason of the high performance of background was on account of the signal probe alone can hybridize with S1 residue due to the high affinity even there was no biotin-streptavidin complex generated in the absence of Dam MTase. However, SP2 alone can't form a stable complex because of a relatively short complementary region. If the cleavage of DNA S1/S2 by Mbo I was prevented through methylation, the functional AuNP was tightly captured by DNA S1 on the basis of a biotin-streptavidin complex, which promoted the hybridization between signal probes and the DNA S1 residue. Similar phenomena have also been described in other studies [22, 23]. In the present study, enzyme cleavage protection can induce adhesion of a considerable number of SP2 because of the enrichment effects of AuNP, at the same time a certain number of Fc tags approach to the electrode surface to promote the electron transfer. Therefore, a high performance of signal-to-noise ratio is obtained. Based on these results, SP2 was chosen as an optimal probe.

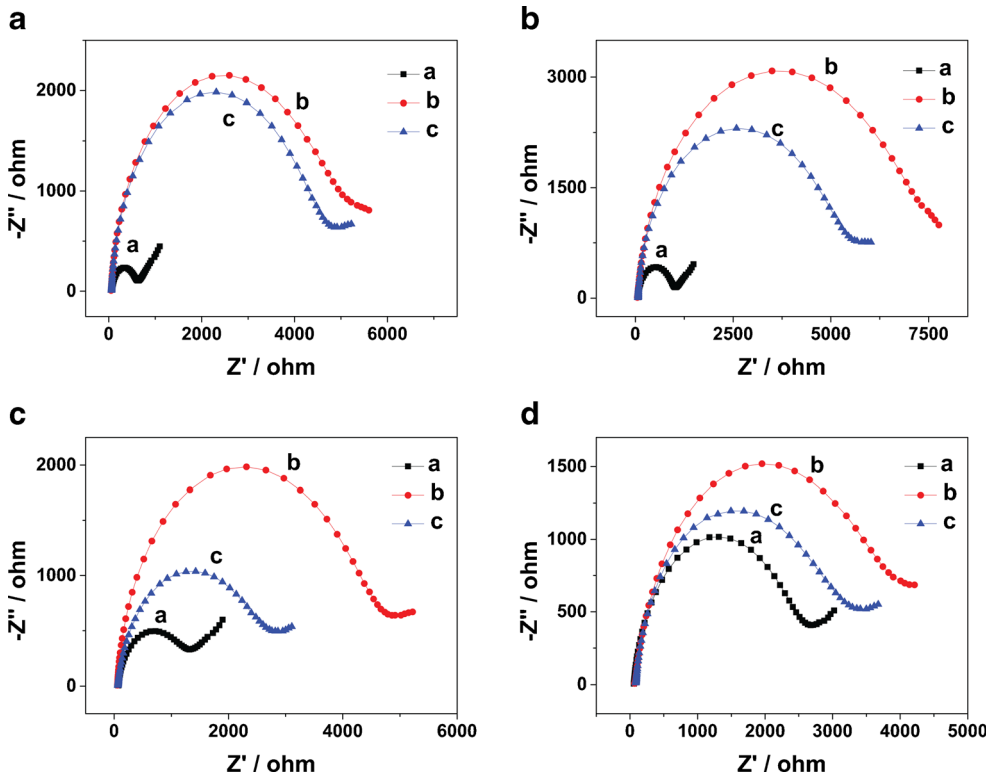

Fig. 2 Optimizations of MCH concentrations. **a** 20 μM; (**b**) 50 μM; (**c**) 100 μM; (**d**) 200 μM

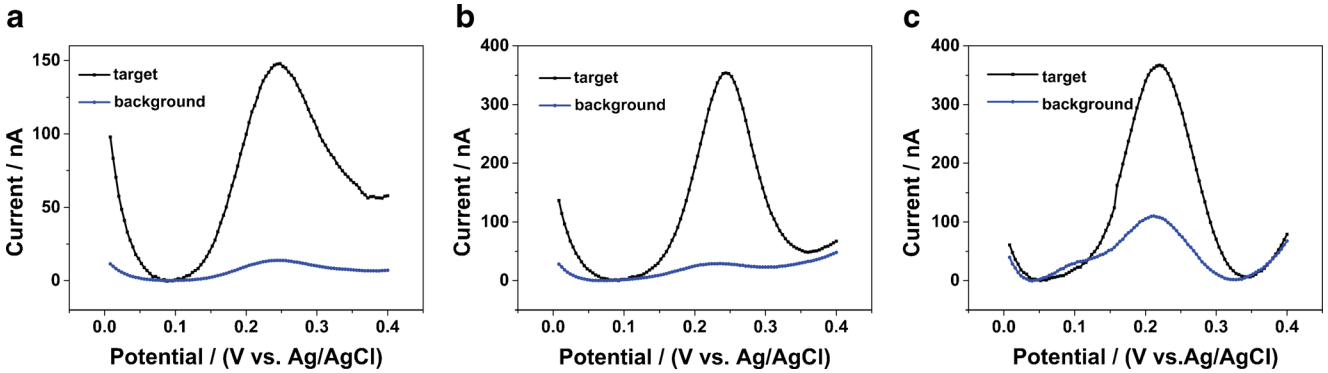

Fig. 3 DPV signals with different signal probes containing (**a**) 6, (**b**) 7, (**c**) 8 bases complementary to S1 residue on the electrodes in the presence and absence of 20 U·mL^{-1} Dam MTase

SAM is a common co-substrate involved in methyl group transfers. The methyl group (−CH3) attached to the methionine sulfur atom in SAM is chemically reactive which allows donation of this group to an acceptor substrate in transmethylation reactions. The effect of SAM concentration therefore has been examined at the range of 0 to 160 μM in this experiment. As seen in Fig. S2a, signal response increased by changing SAM concentration from 0 to 160 μM; the signal slowly increased when SAM concentration exceeded 80 μM. Thus, 80 μM was selected as the optimum concentration for SAM in the following experiments.

As shown in Fig. S2b, current intensity was reduced and reached the minimum value of 50 U·mL^{-1} as Mbo I concentration increased. Thus, 50 U·mL^{-1} of Mbo I was selected for the sensing procedure.

Performance of the biosensor

To assess the performance of the present biosensor, a series of Dam MTase at different concentrations were prepared and DPV was conducted to record the response currents. As shown in Fig. 4, the peak currents were dynamically upregulated as target concentration increased from 0.05 to 50 U·mL^{-1}. A good linear relationship was observed between peak current and target logarithm concentration ranging from 0.1 to 40 U·mL^{-1} was achieved. The peak currents that responded to the target at higher or lower concentrations were beyond the linear response range. The linear regression equation was I (nA)=104.9 Log_{10}C (U·mL^{-1})+219.2, with a correlation coefficient of 0.9987 (R^2) and the detection limit reaches 0.024 U·mL^{-1} (S/N=3). The analytical performance of our biosensor was compared with that described in previous studies. (See Table 2) [11, 31–34]. Table 2 shows that the established biosensor displayed an acceptable analytical range and a relatively low detection limit. This ultrahigh sensitivity may be attributed to several factors. First, the insertion method with a passive gold electrode not only resulted in a more uniform DNA but also provided a sufficient space for endonuclease digestion. Second, AuNP yielded a high surface to volume ratio to carry more signal probe; thus, more Fc tags can be used label electrode surface, even very little Dam MTase was introduced. This procedure greatly enhanced the signal response. Third, a signal probe containing different amounts of nucleotides complementary to DNA S1 residue was optimized to obtain a high signal to noise ratio. Using this strategy, we can drag Fc moieties closer to the electrode, promoting electron transfer and further enhance the signal intensity. Furthermore, the DNA S1 residue left on the electrode after digestion of enzyme acted as a fixer for the hybridization to SP, thus avoid the need of adding additional exogenous adjunct probes and making the best use of the product derived from DNA S1/S2 cleavation.

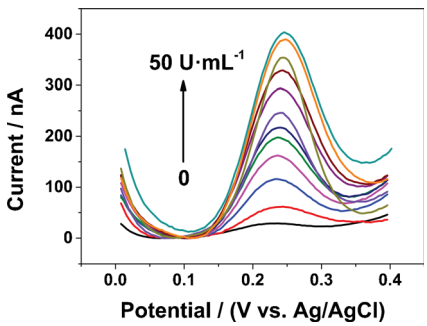

Fig. 4 DPV responses of the sensing system to Dam MTase at varying concentrations. From bottom to top: 0, 0.05, 0.1, 0.25, 0.5, 1, 2, 5, 10, 20, 40 and 50 U·mL^{-1}

Table 2 Comparison of different DNA biosensors for determination of methyltransferases

Method	Linear range (U·mL^{-1})	Detection limit (U·mL^{-1})	Reference
Fluorescent	0.1–4	0.06	[11]
Fluorescent	0.5–100	0.1	[31]
Electroluminescence	1–50	0.33	[32]
Colorimetry	2–32	0.5	[33]
Electrochemistry	0.1–40	0.03	[34]
Electrochemistry	0.1–40	0.024	This work

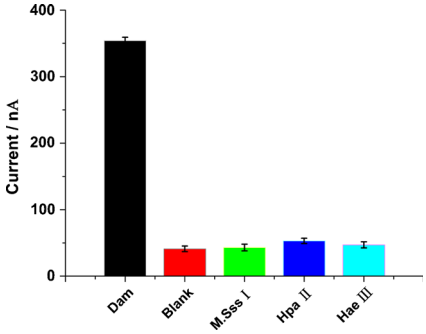

Fig. 5 Specificity investigation of different methyltransferases

Stability, reproducibility, recovery tests and selectivity

In this study, the relative standard deviation (RSD) of the current signal at 40 U·mL^{-1} Dam MTase of the obtained biosensor was less than 4.18 % for six modified electrodes prepared at the same conditions. The current response at 40 U·mL^{-1} MTase retained more than 98 % of its original response after 7 days and 93.6 % after 30 days, during storage at 4 °C. The good reproducibility and stability is largely attributed to the strong biotin-streptavidin bond and high stability of AuNP. The recovery tests for MTase were performed through the standard addition method, which through adding Dam MTases of different known concentrations into fetal bovine serum (diluted 10-fold). The calculated recovery values were in the range of 99.4–102.2 % and shown in Table S3, indicating that the biosensor may be of great value for Dam MTase assay in complicated environments.

To evaluate the selectivity of this sensing system, M.Sss I, Hpa II, and Hae III MTases were interrogated under identical conditions. As shown in Fig. 5, the current signal showed no change in the presence or absence of M.Sss I, Hpa II, and Hae III, indicating outstanding specificity and selectivity against other MTases of this biosensor.

Conclusion

Here, we have developed a signal-on biosensor for the highly sensitive detection of Dam MTase using insertion approach instead of backfilling approach which can enhance the biosensor performance via giving efficient space for methyltransferase. With the combination of methylation-resistance restriction endonuclease cleavage and dragging strategy to bring the Fc labeled reporter close to the electrode. By taking advantage of these strategies as well as the enrichment effect of AuNPs, it enables the assay of MTase activity with an impressive detection limit as low as 0.024 U·mL^{-1}, much lower than those of most existing methods. Owing to the specific site recognition of MTases, this new platform can discriminate Dam MTase from other MTases such as M.Sss I, Hpa II and Hae III with high selectivity. This simple strategy can be used to detect other methyltransferase specificity by simply change the sequence and has high potential use in biological process researches as well as clinical diagnostics.

Acknowledgments This work was financially supported by the Natural Science Research Foundation of China (81171415) and the science & technology bureau of Yibin (2014SF015).

References

1. Heithoff DM, Sinsheimer RL, Low DA, Mahan MJ (1999) An essential role for DNA adenine methylation in bacterial virulence. Science 284(5416):967–970
2. Robertson KD (2005) DNA methylation and human disease. Nat Rev Genet 6(8):597–610
3. Matzke MA, Mosher RA (2014) RNA-directed DNA methylation: an epigenetic pathway of increasing complexity. Nat Rev Genet 15(6):394–408
4. Hansen RS, Wijmenga C, Luo P, Stanek AM, Canfield TK, Weemaes CM, Gartler SM (1999) The DNMT3B DNA methyltransferase gene is mutated in the ICF immunodeficiency syndrome. Proc Natl Acad Sci 96(25):14412–14417
5. Richardson B, Scheinbart L, Strahler J, Gross L, Hanash S, Johnson M (1990) Evidence for impaired T cell DNA methylation in systemic lupus erythematosus and rheumatoid arthritis. Arthritis Rheum 33(11):1665–1673
6. Das PM, Singal R (2004) DNA methylation and cancer. J Clin Oncol 22(22):4632–4642
7. Jurkowska RZ, Ceccaldi A, Zhang Y, Arimondo PB, Jeltsch A (2011) DNA methyltransferase assays. In: Epigenetics protocols. Springer, pp 157–177
8. Herman JG, Graff JR, Myöhänen S, Nelkin BD, Baylin SB (1996) Methylation-specific PCR: a novel PCR assay for methylation status of CpG islands. Proc Natl Acad Sci 93(18):9821–9826
9. Zhang Y, Rohde C, Tierling S, Stamerjohanns H, Reinhardt R, Walter J, Jeltsch A (2009) DNA methylation analysis by bisulfite conversion, cloning, and sequencing of individual clones. In: DNA Methylation. Springer, pp 177–187
10. Johnston JW, Harding K, Bremner DH, Souch G, Green J, Lynch PT, Grout B, Benson EE (2005) HPLC analysis of plant DNA methylation: a study of critical methodological factors. Plant Physiol Biochem 43(9):844–853
11. Zhao C, Qu K, Song Y, Ren J, Qu X (2011) A universal, label-free, and sensitive optical enzyme-sensing system for nuclease and methyltransferase activity based on light scattering of carbon nanotubes. Adv Funct Mater 21(3):583–590
12. Zhao Y, Chen F, Wu Y, Dong Y, Fan C (2013) Highly sensitive fluorescence assay of DNA methyltransferase activity via methylation-sensitive cleavage coupled with nicking enzyme-assisted signalamplification. Biosens Bioelectron 42:56–61
13. Li W, Liu Z, Lin H, Nie Z, Chen J, Xu X, Yao S (2010) Label-free colorimetric assay for methyltransferase activity based on a novel methylation-responsive DNAzyme strategy. Anal Chem 82(5): 1935–1941
14. Li W, Wu P, Zhang H, Cai C (2012) Signal amplification of graphene oxide combining with restriction endonuclease for site-specific determination of DNA methylation and assay of methyltransferase activity. Anal Chem 84(17):7583–7590
15. Hlavata L, Striesova I, Ignat T, Blaskovisova J, Ruttkay-Nedecky B, Kopel P, Adam V, Kizek R, Labuda J (2015) An electrochemical DNA-based biosensor to study the effects of CdTe quantum dots on UV-induced damage of DNA. Microchim Acta 182(9-10):1715–1722

16. Jing X, Cao X, Wang L, Lan T, Li Y, Xie G (2014) DNA-AuNPs based signal amplification for highly sensitive detection of DNA methylation, methyltransferase activity and inhibitor screening. Biosens and Bioelectron 58:40–47
17. Wang C, Zhang L, Guo Z, Xu J, Wang H, Zhai K, Zhuo X (2010) A novel hydrazine electrochemical sensor based on the high specific surface area graphene. Microchim Acta 169(1–2):1–6
18. Liu T, Chen X, Hong C-Y, Xu X-P, Yang H-H (2014) Label-free and ultrasensitive electrochemiluminescence detection of microRNA based on long-range self-assembled DNA nanostructures. Microchim Acta 181(7–8):731–736
19. Fang X, Jiang W, Han X, Zhang Y (2013) Molecular beacon based biosensor for the sequence-specific detection of DNA using DNA-capped gold nanoparticles-streptavidin conjugates for signal amplification. Microchim Acta 180(13–14):1271–1277
20. Drummond TG, Hill MG, Barton JK (2003) Electrochemical DNA sensors. Nat Biotechnol 21(10):1192–1199
21. Josephs EA, Ye T (2013) Nanoscale spatial distribution of thiolated DNA on model nucleic acid sensor surfaces. ACS Nano 7(4):3653–3660
22. Hu J, Yu Y, Brooks JC, Godwin LA, Somasundaram S, Torabinejad F, Kim J, Shannon C, Easley CJ (2014) A reusable electrochemical proximity assay for highly selective, real-time protein quantitation in biological matrices. J Am Chem Soc 136(23):8467–8474
23. Qiu L, Qiu L, Wu Z-S, Shen G, Yu R-Q (2013) Cooperative amplification-based electrochemical sensor for the zeptomole detection of nucleic acids. Anal Chem 85(17):8225–8231
24. Haiss W, Thanh NT, Aveyard J, Fernig DG (2007) Determination of size and concentration of gold nanoparticles from UV-vis spectra. Anal Chem 79(11):4215–4221
25. Jin R, Wu G, Li Z, Mirkin CA, Schatz GC (2003) What controls the melting properties of DNA-linked gold nanoparticle assemblies? J Am Chem Soc 125(6):1643–1654
26. Li J, Chu X, Liu Y, Jiang J-H, He Z, Zhang Z, Shen G, Yu R-Q (2005) A colorimetric method for point mutation detection using high-fidelity DNA ligase. Nucleic Acids Res 33(19):e168
27. Liu J, Lu Y (2006) Preparation of aptamer-linked gold nanoparticle purple aggregates for colorimetric sensing of analytes. Nat Protoc 1(1):246–252
28. Nam J-M, Thaxton CS, Mirkin CA (2003) Nanoparticle-based bio-bar codes for the ultrasensitive detection of proteins. Science 301(5641):1884–1886
29. Müller WD, Nascimento ML, Zeddies M, Córsico M, Gassa LM, Mele MAFL (2007) Magnesium and its alloys as degradable biomaterials: corrosion studies using potentiodynamic and EIS electrochemical techniques. Maters Res 10(1):5–10
30. Zuker M (2003) Mfold web server for nucleic acid folding and hybridization prediction. Nucleic Acids Res 31(13):3406–3415
31. Ouyang X, Liu J, Li J, Yang R (2011) A carbon nanoparticle-based low-background biosensing platform for sensitive and label-free fluorescent assay of DNA methylation. Chem Commun 48(1):88–90
32. Yang Z, Wang F, Wang M, Yin H, Ai S (2014) A novel signal-on strategy for M. SssI methyltransfease activity analysis and inhibitor screening based on Photoelectrochemical immunosensor. Biosens Bioelectron 66:109–114
33. Wu Z, Z-K W, H T, Tang L-J, Jiang J-H (2013) Activity-based DNA-gold nanoparticle probe as colorimetric biosensor for DNA methyltransferase/glycosylase assay. Anal Chem 85(9):4376–4383
34. Xu Z, Yin H, Tian Z, Zhou Y, Ai S (2014) Electrochemical immunoassays for the detection the activity of DNA methyltransferase by using the rolling circle amplification technique. Microchim Acta 181(3–4):471–477